



Small Island Developing States under threat by rising seas even in a 1.5 °C warming world

Received: 1 May 2023

Accepted: 7 September 2023

Published online: 9 October 2023

 Check for updates

Michalis I. Vousdoukas^{1,2}, Panagiotis Athanasiou³, Alessio Giardino⁴, Lorenzo Mentaschi⁵, Alessandro Stocchino^{6,7}, Robert E. Kopp^{8,9}, Pelayo Menéndez¹⁰, Michael W. Beck¹⁰, Roshanka Ranasinghe^{3,11,12} & Luc Feyen¹³

Small Island Developing States (SIDS) have long been recognized as some of the planet's most vulnerable areas to climate change, notably to rising sea levels and coastal extremes. They have been crucial in raising ambitions to keep global warming below 1.5 °C and in advancing the difficult debate on loss and damage. Still, quantitative estimates of loss and damage for SIDS under different mitigation targets are lacking. Here we carry out an assessment of future flood risk from slow-onset sea-level rise and episodic sea-level extremes along the coastlines of SIDS worldwide. We show that by the end of this century, without adaptation, climate change would amplify present direct economic damages from coastal flooding by more than 14 times under high-emissions scenarios. Keeping global warming below 1.5 °C could avoid almost half of unmitigated damage, depending on the region. Achieving this climate target, however, would still not prevent several SIDS from suffering economic losses that correspond to considerable shares of their GDP, probably leading to forced migration from low-lying coastal zones. Our results underline that investments in adaptation and sustainable development in SIDS are urgently needed, as well as dedicated support to assisting developing countries in responding to loss and damage due to climate change.

Rising sea levels¹ together with changing weather patterns² are expected to affect coastal communities worldwide³. Collectively, Small Island Developing States (SIDS) defines a group of countries located in the Caribbean Sea, East Atlantic, and Pacific and Indian Oceans, and are home to ~70 million people (see Table 1 for the list of countries and regions). Already from the 1990s and the Intergovernmental Panel on Climate Change (IPCC) First Assessment Report⁴, Small Islands

have been identified as some of the most vulnerable regions to climate change⁵ due to the large proportions of people, assets and infrastructure necessarily located in the coastal zone⁶, compounded by economic, technological, social and ecological barriers to adaptation⁷.

Despite their similarities in terms of climate vulnerability to coastal flooding, the 52 to 60 (depending on the definition) SIDS exhibit large differences among themselves. SIDS include 4 atoll nations

¹Department of Marine Sciences, University of the Aegean, Mitilene, Greece. ²MV Coastal and Climate Research Ltd, Limassol, Cyprus. ³Deltares, Delft, the Netherlands. ⁴Climate Change and Sustainable Development Department, Asian Development Bank, Manila, Philippines. ⁵Department of Physics and Astronomy "Augusto Righi" (DIFA), University of Bologna, Bologna, Italy. ⁶Department of Civil and Environmental Engineering, The Hong Kong Polytechnic University, Kowloon, Hong Kong, China. ⁷State Key Laboratory of Marine Pollution, City University of Hong Kong, Hong Kong, China. ⁸Department of Earth and Planetary Sciences, Rutgers University, New Brunswick, NJ, USA. ⁹Institute of Earth, Ocean, and Atmospheric Sciences, Rutgers University, New Brunswick, NJ, USA. ¹⁰Institute of Marine Sciences, University of California Santa Cruz, Santa Cruz, CA, USA. ¹¹Department of Coastal and Urban Risk and Resilience, IHE Delft Institute for Water Education, Delft, the Netherlands. ¹²Department of Infrastructure Engineering, University of Melbourne, Melbourne, Victoria, Australia. ¹³European Commission, Joint Research Centre (JRC), Ispra, Italy. ✉e-mail: vousdoukas@gmail.com; luc.feyen@ec.europa.eu

Table 1 | List of SIDS countries per region and their GDP (reference year 2015), population and total area, with country names and codes, and membership in the AOSIS

Area	Country	Country code	AOSIS member	GDP (US\$B)	Population (×1,000)	Area (km ²)
Caribbean Sea	Aruba	ABW	No	5.41	117.11	180
	Anguilla	AIA	No	0.32	14.49	78
	Antigua and Barbuda	ATG	Yes	1.30	95.20	440
	Bonaire, Sint Eustatius and Saba	BES	No	1.03	27.07	316
	Bahamas	BHS	Yes	12.33	382.99	10,010
	Belize	BLZ	Yes	3.87	355.92	22,810
	Bermuda	BMU	No	9.38	65.26	54
	Barbados	BRB	Yes	5.39	277.20	430
	Cuba	CUB	Yes	190.19	11,031.29	103,800
	Curacao	CUW	No	5.75	178.96	444
	Cayman Islands	CYM	No	7.00	57.96	240
	Dominica	DMA	Yes	0.45	72.02	750
	Dominican Republic	DOM	Yes	146.85	10,885.17	48,310
	Guadeloupe	GLP	No	7.65	480.34	1,645
	Grenada	GRD	Yes	1.05	107.29	340
	Guyana	GUY	Yes	4.13	762.43	196,850
	Haiti	HTI	Yes	21.75	10,945.28	27,560
	Jamaica	JAM	Yes	33.81	2,791.66	10,830
	Saint Kitts and Nevis	KNA	Yes	0.90	51.86	260
	Saint Lucia	LCA	Yes	1.49	181.00	610
	Saint-Martin	MAF	No	0.76	36.26	50
	Montserrat	MSR	No	0.06	5.09	101
	Martinique	MTQ	No	7.73	417.97	1,117
	Puerto Rico	PRI	No	91.17	3,620.01	8,870
Suriname	SUR	Yes	9.61	563.33	156,000	
Sint Maarten	SXM	No	1.22	40.93	34	
Turks and Caicos Islands	TCA	No	1.45	38.07	950	
Trinidad and Tobago	TTO	Yes	40.28	1,357.62	5,130	
Saint Vincent and the Grenadines	VCT	Yes	0.62	108.73	390	
British Virgin Islands	VGB	No	1.14	26.83	150	
Virgin Islands, US	VIR	No	3.65	98.25	350	
East Atlantic	Cape Verde	CPV	Yes	2.25	552.67	4,030
	Guinea-Bissau	GNB	Yes	1.48	1,842.10	28,120
	Sao Tome and Principe	STP	Yes	0.33	221.52	960
Indian Ocean	Bahrain	BHR	No	64.03	1,861.27	780
	Comoros	COM	Yes	3.26	976.61	1,861
	Maldives	MDV	Yes	2.12	357.87	300
	Mauritius	MUS	Yes	14.01	1,414.77	2,030
	Seychelles	SYC	Yes	4.65	114.39	460
Pacific Ocean	American Samoa	ASM	No	0.91	53.65	200
	Cook Islands	COK	Yes	0.41	16.49	118
	Fiji	FJI	Yes	5.95	896.98	18,270
	Micronesia	FSM	Yes	0.85	111.54	700
	Guam	GUM	No	15.51	198.76	540
	Kiribati	KIR	Yes	0.23	111.75	810
	Marshall Islands	MHL	Yes	0.47	54.34	180
Northern Mariana Islands	MNP	No	2.43	60.44	460	

Table 1 (continued) | List of SIDS countries per region and their GDP (reference year 2015), population and total area, with country names and codes, and membership in the AOSIS

Area	Country	Country code	AOSIS member	GDP (US\$B)	Population (×1,000)	Area (km ²)
	New Caledonia	NCL	No	18.47	287.62	18,280
	Niue	NIU	Yes	0.03	1.58	267
	Nauru	NRU	Yes	0.22	11.56	20
	Palau	PLW	Yes	0.43	18.19	460
	Papua New Guinea	PNG	Yes	43.75	8,093.91	452,860
	French Polynesia	PYF	No	7.17	297.49	3,520
	Singapore	SGP	Yes	333.98	5,706.35	709
	Solomon Islands	SLB	Yes	2.47	647.28	27,990
	Timor-Leste	TLS	Yes	3.87	1,342.42	14,870
	Tonga	TON	Yes	0.59	97.39	720
	Tuvalu	TUV	Yes	0.07	13.08	30
	Vanuatu	VUT	Yes	2.87	287.51	12,190
	Samoa	WSM	Yes	1.68	182.93	2,830

AOSIS, Alliance of Small Island States (<https://www.aosis.org/>).

(that is, Kiribati, Marshall Islands, Tuvalu and Maldives), 14 volcanic islands (that is, Cape Verde, Comoros, Sao Tome and Principe, Dominica, Grenada, Saint Kitts and Nevis, Saint Lucia, Saint Vincent and the Grenadines, Fiji, Papua New Guinea, Samoa, Solomon Islands, Tonga, Vanuatu) and 4 continental countries (Belize, Guinea-Bissau, Guyana, Suriname). Consequently, their coastal ecosystems and geomorphologies are very different. In terms of drivers of coastal flooding, while most SIDS are located in the tropical cyclone (TC) belt, there are a few that hardly experience TCs (for example, Bahrain, Belize, Suriname). Some SIDS are exposed to long-period swell waves (for example, Pacific SIDS), while others mostly experience short-period wind sea waves (for example, Caribbean SIDS). Tides are predominantly microtidal in SIDS. Their economies also vary remarkably, including some of the least developed countries in the world, as well as some of the countries with the highest gross domestic product (GDP) per capita (for example, Singapore). Finally, their land governance structures are diverse, with some of these countries practicing a land tenure system where most of the land is publicly owned or held under customary law, and others where it is privately owned. Thus, the adaptive capacities of different SIDS vary greatly, consequently affecting their present and future vulnerability to coastal flooding. In addition, high temperatures and ocean acidification are known to threaten coral communities and the natural protection they offer⁸.

SIDS already suffer high losses and damage from extreme coastal events and rising seas⁸. In 2019, tropical cyclone Dorian resulted in over US\$3 billion in damages and losses linked to flooding only in the Bahamas, with 30,000 people impacted, 67 fatalities and 282 missing⁹. Tropical cyclone Maria hit Dominica in 2017 and resulted in an economic damage of US\$1.311 billion, or 226% of its 2016 GDP, with 80% of the population affected¹⁰. In the Pacific Solomon Islands and Micronesia, the islands of Hetaheta and Sogomou have lost 62% and 55% of land compared to 1947, while Kale and Rapita have been completely lost¹¹.

There is growing attention on climate risks in SIDS⁵, but studies thus far have mainly focused on a single state¹², group of states¹³ or region¹⁴. The diversity among SIDS in terms of their territorial areas, governance systems, economic development and geographic characteristics, combined with differences in data and methodologies used in local and regional studies, hinders the development of a comprehensive picture of future risks of rising seas and coastal extremes in these vulnerable states. There are global coastal hazard¹⁵ and risk³ assessments that include SIDS, but they either do not perform detailed

assessments¹⁶, or only provide a general overview along coastlines worldwide, without a specific focus on SIDS¹⁷.

Here we present an assessment of coastal flood risk for all SIDS during the present century for scenarios that span from ambitious emissions cuts to very high emissions: '1.5 °C world' (Shared Socio-economic Pathways (SSP)1–1.9), 'low-emissions' (SSP1–2.6), 'moderate emissions' (SSP2–4.5), 'high emissions' (SSP3–7.0) and 'very high emissions' (SSP5–8.5). The modelling framework combines probabilistic dynamic simulations of relative sea-level rise, tides, waves and surges to estimate extreme sea levels (ESLs) along the coastlines of SIDS throughout this century. Land areas permanently inundated and episodically flooded by ESLs were obtained using two-dimensional (2D) hydrodynamic modelling while accounting for artificial flood protection and natural protection afforded by reefs and mangroves. We quantify human exposure and direct economic losses by combining the flood inundation maps with a detailed mapping of exposure (population, land use, GDP per capita) and empirical vulnerability relations (see Methods). Below we discuss median estimates, with confidence ranges listed in brackets (5th–95th percentiles) where appropriate.

Present-day coastal flood loss and damage in SIDS

We estimate that at present and for all SIDS, the expected flooded area (Expected Annual Flooded Area (EAFA), calculated by integration of flooded areas over probability of occurrence of flooding) in a given year is 3,568 (1,460–10,368) km² (Fig. 1e and Supplementary Data Table 1). This corresponds to 0.31% (0.13%–0.94%) of the total SIDS land area. Half of the EAFA is located in the Caribbean Sea and 42% in the Pacific Ocean, with the East Atlantic and the Indian Ocean containing the remaining 5% and 1%, respectively (Fig. 1a,b). However, the region with the highest fraction of its SIDS land area expected to be flooded is the Indian Ocean (0.71%), followed by the East Atlantic (0.61%), Caribbean Sea (0.32%) and Pacific Ocean (0.28%).

The present-day Expected Annual Number of People Exposed (EAPE) to coastal flooding for all SIDS amounts to 131,315 (49,834–415,472), or 0.18% (0.07%–0.58%) of SIDS' total population (Fig. 2a and Supplementary Data Table 4). Approximately 61% of people exposed are in the Caribbean Sea and 22% in the Pacific Ocean, with the highest contribution from Haiti (22%), Papua New Guinea and Cuba (both around 11%). The country with the highest EAPE as a fraction of its total population is Vanuatu (1.96%), followed by Belize (1.59%), while there are also several other countries where the estimated EAPE exceeds 1%

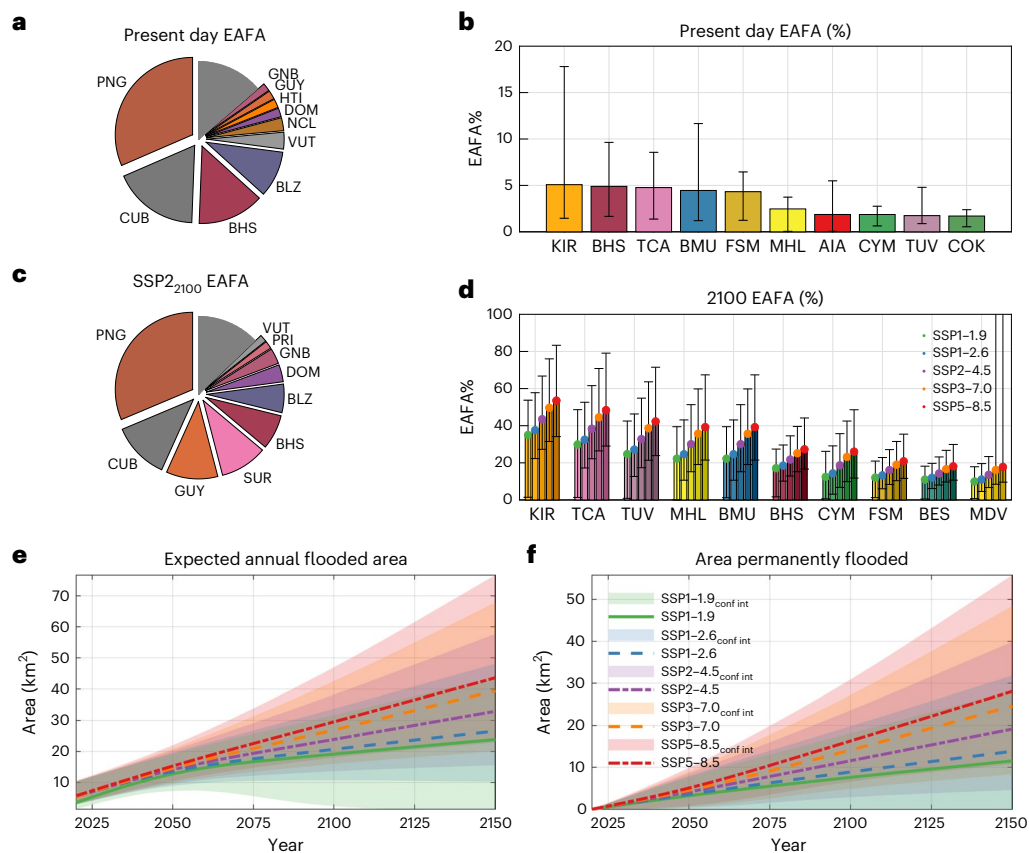


Fig. 1 SIDS will be increasingly exposed to coastal floods until 2150. **a**, Pie plot indicating the countries with the highest share of the total baseline Eafa. Colours in **a–d** are unique for each country and only the countries with the 10 highest values are shown. **b**, Baseline Eafa as a percentage of the country area (median values in bars, black whiskers indicate the 5th–95th confidence intervals). **c**, Pie plot indicating the highest country contributions to the total 2100 Eafa under SSP2–4.5. **d**, Ten countries with the highest 2100 Eafa as a percentage of the country area (median values in circles, black whiskers indicate

the 5th–95th quantile ranges); bars are grouped in stacks of 5, with one each for the 5 scenarios studied: ‘1.5 °C world’ (SSP1–1.9, green), ‘low-emissions’ (SSP1–2.6, blue), ‘moderate-emissions’ (SSP2–4.5, purple), ‘high-emissions’ (SSP3–7.0, orange) and ‘very-high-emissions’ (SSP5–8.5, red). **e, f**, Evolution of Eafa (**e**) and area permanently flooded (**f**) (that is, below the high-tide water level) until the year 2150 under all five scenarios (the lines express the ensemble median projections and the coloured areas the 5th–95th confidence intervals). For country abbreviations, see Table 1.

of the total population (for example, Anguilla, Bahamas, Micronesia, Bermuda and Marshall Islands).

The present-day Expected Annual Damage (EAD) for all SIDS is US\$1.64 (0.69–5.15) billion (2020 values), corresponding to 0.13% (0.06%–0.41%) of SIDS’ total GDP (Figs. 2b and 3f, and Supplementary Data Table 6). Around 96% of the total losses occur in the Caribbean Sea (49%; Fig. 3a) and the Pacific Ocean (46.5%; Fig. 3d), while the region with the highest EAD as a fraction of the GDP is the East Atlantic (1% (0.5%–5.9%); Fig. 3b), even though its absolute values are the lowest among all regions, followed by the Indian Ocean (Fig. 3c). For several SIDS, present average annual coastal flood losses already amount to a considerable portion of their GDP, most notably for Belize (3.17%), Bahamas (1.75%), Vanuatu (1.47%), Turks and Caicos (1.4%) and Papua New Guinea (1.24%; Supplementary Data Table 7).

Climate change-induced coastal flood loss and damage in SIDS

By 2050, the area expected to be flooded per year (Eafa) for all SIDS is projected to more than triple compared with the present-day value and to extend from 14,224 (9,809–19,601) km² for the 1.5 °C world scenario to 15,620 (11,175–21,151) km² for the very-high-emissions scenario (Fig. 1e) and amount to 13,933 (10,628–20,221) for the moderate-emissions scenario. For all scenarios, Eafa expands with time, to reach 23,890 (13,810–38,059) km² by the end of this century for SSP2–4.5,

a number that accounts for 1.1–3.2% of SIDS’ total area. Limiting warming to 1.5 °C would restrain the flooded area in 2100 to 19,213 (1,460–31,697) km², while under the very high-emissions SSP5–8.5 scenario, it would increase to 29,515 (18,330–46,463) km². Part of the land lies below the future high-tide water level and will be subject to regular tidal (or nuisance) flooding, hence any development will be permanently lost unless adequately protected. The median extent of this low-lying land ranges between 7,653 km² for the 1.5 °C scenario to 16,274 km² for the very-high-emissions scenario (Fig. 1f and Supplementary Data Table 3). The increasing trend extends beyond the twenty-first century as Eafa in 2150 is projected to reach 23,845 (1,460–43,873) km² (or 2.2 (0.9–4.0)% of the total area) and 43,625 (22,898–76,657) km² (3.6 (1.9–6.4)%) under SSP1–1.9 and SSP5–8.5, respectively. For the same scenarios, the median area permanently inundated ranges between 11,530 and 28,083 km² or 1.0% and 2.3% of the total area. The SIDS with the highest relative contributions to the total Eafa are similar to the baseline (Fig. 1a,b), but some rankings change, with Bonaire, Sint Eustatius and Saba, as well as the Maldives being added to the list (Fig. 1c,d).

How these projected changes in flood hazard translate into future coastal impacts will depend on local exposure subject to socioeconomic dynamics, including adaptation policy implementation and the development of coastal management plans¹⁸. Because assumptions of demographic and economic developments over long time spans are highly uncertain¹⁹, it is important to single out the effect of climate

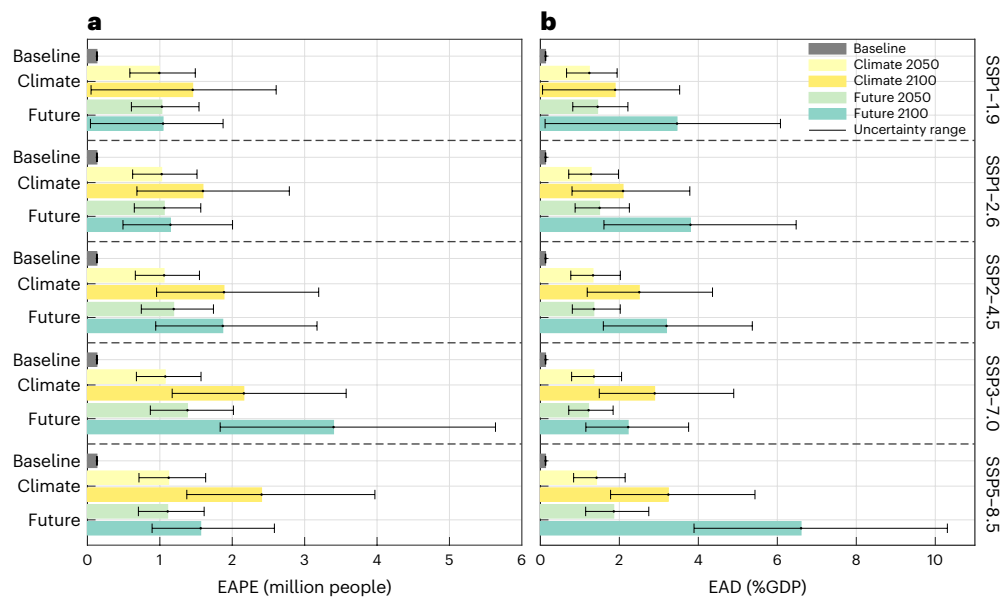


Fig. 2 | Baseline and projected values for EAD and EAPE, and the importance of climatic and socioeconomic drivers. a, b. Estimated EAPE (a) and EAD as a percentage of the GDP (b) under the ‘1.5 °C world’ (SSP1-1.9), ‘low-emissions’ (SSP1-2.6), ‘moderate-emissions’ (SSP2-4.5), ‘high-emissions’ (SSP3-7.0) and ‘very-high-emissions’ (SSP5-8.5) scenarios. Baseline in greyscale; only climate

change with static economy in yellow; and the combined effect of climatic and socioeconomic dynamics in green. Lighter and darker coloured bars indicate estimates in 2050 and 2100, respectively. The bars represent the median results and the black whiskers indicate the 5th–95th confidence intervals.

change and therefore, here we first impose the flood hazard projections on present (2020) population and economy.

Given that nearshore areas tend to be densely populated with growing levels of informal urbanism⁶, the projected increase in population exposed outpaces that in the projected size of flooded area. By mid-century, ~5 times more people will be flooded compared with present day for the lowest emissions scenario (SSP1-1.9) and nearly 7 times as many under the very high-emissions scenario (SSP5-8.5) (Fig. 2a and Supplementary Data Table 4). By 2100, the number of people exposed to flooding in a given year further increases for all scenarios and is projected to amount to nearly 1.45 million (49,834–2,598,672) (2.2% of SIDS population, ~10-fold of today) with 1.5 °C warming. The same number reaches 1.88 million (951,383–3,184,341) for SSP2-4.5 and 2.4 million (1,368,081–3,958,061) for SSP5-8.5. By 2150, EAPE is projected to reach 1,875,817 (49,834–3,719,588) and 3,696,801 (1,788,618–6,530,437) under SSP1-1.9 and SSP5-8.5, respectively.

Flood damage is projected to increase even more dramatically than population exposed, with estimated EAD by mid-century being 9 to 11 times the present-day damages. We project that by the end of this century, due to climate change only, average annual damages from coastal flooding in SIDS will further grow to US\$23.8 (0.7–44.3), US\$31.5 (14.9–54.7) and US\$40.7 (22.3–68.2) billion for the SSP1-1.9, SSP2-4.5 and SSP5-8.5 scenarios, respectively (Fig. 3f and Supplementary Data Table 6). This corresponds to 1.89% (0.06%–3.53%), 2.5% (1.19%–4.36%) and 3.24% (1.78%–5.43%) of SIDS’ total GDP (Fig. 2b). For the same scenarios and the year 2150, EAD increases even further to reach US\$31.4 (0.7–64.3), US\$46.3 (17.8–85.2) and US\$63.9 (29.8–111.5) billion, respectively, with the median values corresponding to 2.5%, 3.7% and 5.1% of the GDP. Such high increase in economic impacts is driven by the expansion of the flooded areas, but also by higher flood depths that cause more damage per unit area. Overall, regional, total and AOSIS (Fig. 3e) EAD estimates follow similar trends.

At a more granular level, flood exposure and losses vary substantially among regions and countries. By the end of the century, each year 0.9 to 1.7 million people will be exposed (EAPE) to flooding in the 31 SIDS of the Caribbean Sea, corresponding to 2.0–3.6% of

their population and to a 10- to 18-fold increase compared with the present day. In this region, damages from coastal flooding will be 15 (SSP1-1.9) to 28 (SSP5-8.5) times those of today by 2100, with EAD amounting to US\$13.2 billion under 1.5 °C warming, US\$18.2 billion under SSP2-4.5 and US\$21.44 billion under SSP5-8.5 (Fig. 3a). For the two high-emissions scenarios (SSP3-7.0 and SSP5-8.5), EAD will exceed US\$2 billion per year in Cuba, Puerto Rico and Guyana by 2100, with at least one third of the countries in this region experiencing two orders of magnitude or higher rise in damages by the end of the century compared with present day. Limiting global warming to 1.5 °C by 2100 would still result in >100-fold increases in EAD in Saint Kitts and Nevis, Saint-Martin, the US Virgin Islands, Trinidad and Tobago, Barbados, Guadeloupe and Bermuda. Relative to the size of the present economy, impacts will be highest in Guyana (38% for SSP1-1.9, 64% for SSP5-8.5), Turks and Caicos (39–61%) and Suriname (20–40%).

In the 21 SIDS of the Pacific Ocean, the number of people exposed to coastal flooding is projected to increase 4.5 to 7 times by 2100, corresponding to 1.2–2.0% of the population in this region. Damages by the same time will range between US\$6.6 million (SSP1-1.9) and US\$10.7 billion (SSP5-8.5) (Fig. 3d), or 1.4% and 2.2% of GDP, respectively, of the Pacific Ocean SIDS. More than 50% of the damages for this region will occur in Papua New Guinea and 14% in Singapore. Under moderate emissions (SSP2-4.5), damages rise by at least two orders or more in Tuvalu, Kiribati, Bahrain, Nauru, American Samoa and Singapore. For Singapore, damages remain relatively limited compared with the size of its economy (<1% of GDP) due to its wealth and higher protection standard compared with other SIDS. However, for less prosperous islands such as Tuvalu (48% for SSP1-1.9, 71% for SSP5-8.5), Marshall Islands (27–43%) and Kiribati (15–29%), damages are projected to grow to considerable shares of GDP.

The 5 SIDS located in the Indian Ocean show the highest rise among the regions, with 13 (1.5 °C world) to 17 (very high emissions) times more people exposed by 2100 compared with present day, while damages are projected to become 113 to 152 times higher (Fig. 3c). More than 60% of population exposed and 70% of damages will be in Bahrain, while damages will grow by more than two orders of magnitude in all islands

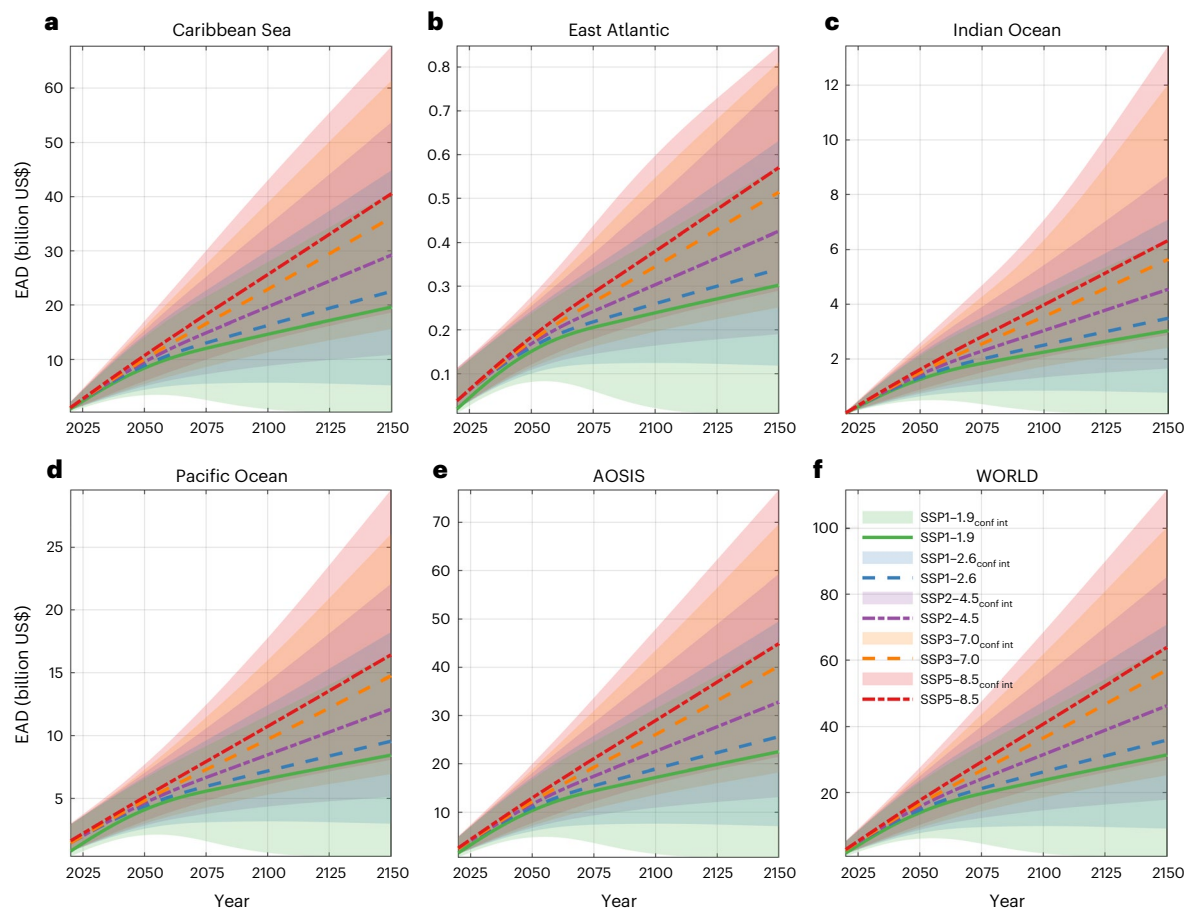


Fig. 3 | Projected evolution of direct economic impacts due to coastal flooding in SIDS. a–f, EAD aggregated at regional (a, Caribbean Sea; b, East Atlantic; c, Indian Ocean; d, Pacific Ocean); e, AOSIS members, as well as at global level (f) under ‘1.5 °C world’ (SSP1–1.9, green), ‘low-emissions’ (SSP1–2.6,

blue), ‘moderate-emissions’ (SSP2–4.5, purple), ‘high-emissions’ (SSP3–7.0, orange) and ‘very-high-emissions’ (SSP5–8.5, red). The lines indicate the median projections and the coloured areas the 5th–95th confidence intervals. Estimates not considering socioeconomic dynamics are presented.

apart from the Seychelles. These increases in flooding are projected to lead to economic losses of 2.4% (SSP1–1.9) to 4.3% (SSP5–8.5) of GDP in Bahrain and 9.2% to 12.5% in the Maldives. Population exposure (90%) and damages (>70%) in Guinea-Bissau dominate the total flood impacts of the 3 SIDS in the East Atlantic, with EAD ranging from 5.4% to 8.6% of GDP under 1.5 °C warming and very high emissions, respectively.

Our analysis shows that avoiding very high emissions (that is, according to SSP5–8.5) and reducing them to moderate levels (that is, according to SSP2–4.5) will result in mitigation of the end-of-century coastal flood damage for SIDS by 23% (Fig. 4); such benefits are projected to increase beyond the twenty-first century, reaching 27.5% in 2150. The effect of such mitigation policies varies regionally depending on the geographical characteristics of SIDS. It is stronger for the India Ocean (24%; Fig. 4c), followed by the Caribbean (23%; Fig. 4a), the East Atlantic (19%; Fig. 4d) and the Pacific Ocean SIDS (19%; Fig. 4b). Benefits of mitigating further to stay below 1.5 °C global warming include an additional reduction in EAD of 24.5% and 30.2% in the years 2100 and 2150, respectively. Countries that would benefit most from mitigation in terms of relative reduction in damages by 2100 are Barbados, Cayman Islands, Dominica, Saint Lucia, Northern Mariana Islands, Puerto Rico, Singapore, Suriname, Trinidad and Tobago, for which total mitigation benefits (that is, comparison between SSP5–8.5 and SSP1–1.9; Fig. 4) exceed 55%. Most of the above SIDS are low-lying islands where ESL reduction implies a higher reduction of flooded areas compared with steeper landscapes; for example, the lowest mitigation benefits are projected for some steep volcanic islands such as American

Samoa, Tonga and French Polynesia. Exceptions are low-lying islands such as Tuvalu and the Maldives, which are severely affected islands under all scenarios but with differences in projected damage among SSPs being smaller than in other SIDS due to their most valuable assets being already exposed to flooding even under low emissions.

By the end of the 22nd century and under SSP1–2.6, the mean sea-level rises by 0.26–1.92 m and EAFA for all SIDS ranges between 7,515 and 24,711 km² (Supplementary Data Table 10), values which correspond to 0.6%–2% of the total SIDS area. By the end of the twenty-third century, sea-level rise (SLR) is projected to even exceed 3.1 m and similar estimates rise to 8,141–35,554 km² and 0.7–2.9%. The upper limit of the SLR projections likely range under very high emissions (SSP5–8.5) exceeds 9 and 16 m by the end of the twenty-second and the twenty-third century, respectively. Such mean sea levels come with high uncertainty but would result in at least 6% of all SIDS area annually flooded, with some islands severely affected (for example, Tuvalu, Marshall Islands, Cayman Islands, Bahamas and the Maldives).

Impacts of rising seas under future socioeconomic conditions

When combining the flood hazard projections in view of climate change together with scenarios of population and economy (see Methods), EAPE for SSP1–2.6 is 28% lower compared with when only accounting for climate change (Fig. 2a). This reflects the decline in SIDS population projected under SSP1, from 71 million at present to 54 million by 2100. The same mechanism drives a 35% reduction in EAPE for SSP5–8.5.

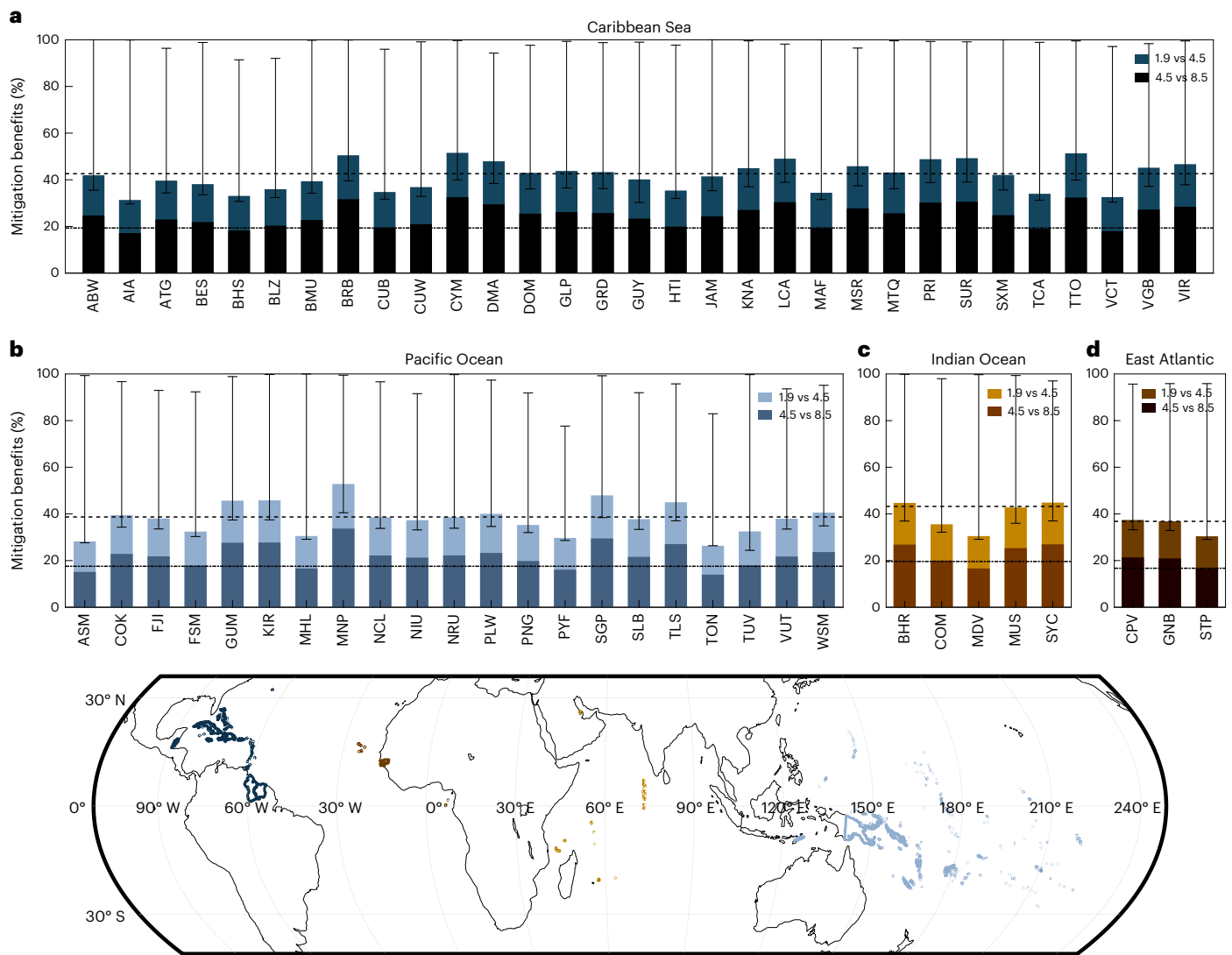


Fig. 4 | Greenhouse gas emissions mitigation reduces coastal flood losses in SIDS. Percent reduction of the EAD on coastal flooding in 2100 between very high (SSP5–8.5) and moderate emissions (SSP2–4.5) scenarios (darker bars), and between moderate emissions (SSP2–4.5) and 1.5°C warming (SSP1–1.9) scenarios (lighter bars). Results at country level for each of the four regions (a, Caribbean Sea; b, East Atlantic; c, Indian Ocean; d, Pacific Ocean). Bars indicate

the ensemble median country-level values, and the black whiskers indicate the 5th–95th confidence ranges. The horizontal lines show the corresponding median mitigation effect at regional level (solid line from SSP2–4.5 to SSP1–1.9, dashed line from SSP2–4.5 to SSP1–1.9). The bottom map highlights the four regions as dark blue (Caribbean), light blue (Pacific), light brown (Indian) and dark brown (East Atlantic). For country abbreviations, see Table 1.

On the contrary, the projected increase in SIDS population and migration towards coastal zones under SSP3–7.0 drive an additional increase in EAPE of 57% by 2100. SIDS in the Indian Ocean show the highest increase in the proportion of the population that lives in coastal flood-prone areas, followed by the Pacific Islands. Even for the SSP1–2.6 scenario, 34% and 11% more people are projected to live near the coast in the Indian and Pacific Oceans, respectively, while in the Caribbean and East Atlantic, the population in coastal low-lying areas are projected to decrease by 30% under this scenario.

Economic growth amplifies damages for all scenarios, with the 2100 EAD projected to reach US\$128.3 (4.4–225.3) (SSP1–1.9), US\$140.9 (59.7–240.1) (SSP1–2.6), US\$133.5 (66.6–224.3) (SSP2–4.5), US\$81.48 (42.2–137.9) (SSP3–7.0) and US\$337.2 (198.8–526.4) (SSP5–8.5) billion, a multi-fold increase from present-day estimated damage of US\$1.64 billion (Fig. 2b). The stronger economic growth projected for SSP2 compared with SSP3 results in the highest absolute damage in SSP2–4.5, despite the smaller increase in ESLs for this scenario

compared with SSP3–7.0. For SSP5–8.5, higher SLR projections coincide with higher asset values as GDP increases and population decreases, resulting in 2100 EAD estimates that are almost 2.5 times higher than for SSP2–4.5. Relative to the size of the economy in 2100, these estimates correspond to 3.5 (SSP1–1.9), 3.8 (SSP1–2.6), 3.2 (SSP2–4.5) and 6.6% (SSP5–8.5) of SIDS’ GDP, or 82%, 81%, 27% and 104% higher, respectively, compared with when only the effects of climate change are accounted for. This is due to the concentration of people, infrastructure and wealth in coastal zones, all of which are projected to intensify in most countries, especially in the Pacific and the Caribbean. The only exception is SSP3–7.0, for which EAD as a fraction of the GDP is 22% lower than when static economy is considered.

Discussion

Despite being highly vulnerable to the effects of climate change, SIDS are among the least-studied regions of the planet²⁰. This study presents a comprehensive assessment of flood risk along coastlines of all SIDS.

We integrate state-of-the-art global modelling tools and datasets with notable improvements on several aspects, such as the accuracy of the digital elevation model, accounting for wave and tropical cyclone effects, nonlinear interactions between water-level components, attenuation of ESLs by reefs and mangroves, and applying 2D hydraulic flood inundation modelling. The spatial and temporal scales considered, however, impose some inevitable epistemic, computational and data limitations (see also Limitations in Methods), therefore our results should be considered as a first-pass global-scale assessment that gives insights on spatial patterns of future coastal flood impacts in SIDS and identifies potential hotspots of impacts of climate change. The present findings should not be directly used for adaptation decision-making at local scales, for which more detailed local-scale assessments are needed.

Coastlines of SIDS host a variety of environments, from low-lying coral atolls to steep rocky coasts. Nearshore waves and currents and thus ESLs are modulated by the nearshore bathymetry and topography. Improvements in the quality and availability of spatial topo-bathymetric data would substantially benefit coastal flood risk modelling^{12,21}, allowing better representation of complicated hydrodynamic processes, in particular at open complex coastlines, such as around temperate rocky coasts and coral reefs that surround many SIDS^{22–24}.

Anthropogenic factors are key drivers of shoreline change worldwide²⁵, and human interventions modulate the impact of extreme weather events by affecting the different flood risk components (hazard, exposure and vulnerability). The bathymetry and topography acts as natural protection, attenuating incoming wave energy, but such capacity depends on its long-term evolution which is difficult to predict²⁶. Similarly, numerical modelling studies have shown that the extent to which rising seas will affect nearshore hydrodynamics depends on whether societies will decide to ‘hold the line’ or let shoreline retreat²⁷. A limited number of states are already planning to further enhance coastal protection in response to SLR²⁸, but these efforts are still local. It has been demonstrated that the interplay between hazard and vulnerability is complex²⁹, and despite the increasing frequency of extreme events, risk reduction efforts have been successful in reducing vulnerability and flood risk³⁰.

All the above interactions depend on multiscale economic, social and political conditions³¹, which are beyond the scope of the present study restricted to assessing coastal flood impacts for SIDS assuming static vulnerability and no improvement in existing natural and artificial coastal protection. This includes the inherent assumption that ecosystems will retain their natural protection capacity in the future, but for this to be the case, they should be properly managed and protected against intensifying stressors³². Recent IPCC reports⁸ underline that coral bleaching will severely affect coral habitats even under 1.5 °C warming and beyond the year 2040, but a recent study leaves some hope that ecosystems could at least adapt if we achieve such a temperature goal³³. The fact is that we are still developing tools that will allow us comprehensive quantitative projections of reef and mangrove evolution, and the absence of such information is an inevitable limitation of studies such as ours. Here we assume that ecosystems will continue to provide natural protection, based also on the fact that as part of the management of natural defences, governments are deciding to purchase insurance to protect reefs from storm damages and to invest in national disaster recovery funding for reef restoration to protect coastal populations³⁴. At the same time, we need to highlight that the above assumption renders our results more conservative and in case ecosystems will not be preserved, future floods will result with even higher impacts.

SIDS have played an important role in international climate discussions to promote the curbing of global warming and implement mechanisms to address loss and damage³⁵ that are not avoided through mitigation and adaptation³⁶. Our findings corroborate the urgency of adapting to slow-onset SLR and associated intensified extreme

coastal events expressed by these vulnerable countries. Even under a stringent mitigation scenario, coastal flood risk in SIDS is projected to increase by more than an order of magnitude by the end of this century. For several SIDS, the costs of future coastal flooding will be very high relative to the size of their economy (for example, Guyana, Turks and Caicos, the Marshall Islands, Guinea-Bissau, Suriname, Kiribati, Belize and Tuvalu). Local flood risk could be further amplified by growing levels of informal urbanism where people and communities settle in highly exposed locations⁶.

Substantial adaptation efforts will therefore be required to mitigate coastal flood impacts. To keep economic damages in 2100 at today’s levels, existing natural and artificial protection would need to be upgraded to withstand rises of extreme sea levels by more than a metre in several countries and under the high-emission scenarios (Supplementary Data Table 11). Countries with the highest estimates of additional protection needed are American Samoa, Samoa, Cook Islands, Cuba, Cayman Islands, Micronesia, Jamaica, Saint-Martin, Aruba, Mauritius and Nauru. Built infrastructure may be cost effective in areas with highly valued assets³⁷, yet is expensive and can have negative effects on biodiversity³⁸. Therefore, effective management of existing natural defences can serve as a cost-effective and less intrusive adaptation option³⁹, but further research is needed regarding their costs and benefits⁴⁰, and the extent to which they can absorb the effects of higher-end SLR⁴¹ and other climatic changes (for example, increasing marine heat waves, ocean acidity). Retreat from low-lying coastal zones in SIDS can be considered either proactively or as an ultimate measure (for example, as a result of failed adaptation, or as a loss and damage response), but can often be hampered by social and ethical challenges and may even be impossible in several islands with limited high-elevation land⁴².

Beyond the twenty-first century, there is strong incentive for climate mitigation as under higher emissions, extreme sea levels could increase by several more metres, threatening the more low-lying islands. The implementation of adaptation in SIDS is further compounded by the lack of resources, governance issues and limited institutional capacity⁷. Major political decisions need to be taken, notably on financing for loss and damage to support vulnerable communities around the world to avert, minimize and address loss and damage from climate change.

Methods

Coastal flood risk modelling framework

We assessed impacts from SLR and episodic flooding along coastlines of SIDS during the twenty-first century, considering both permanent inundation from SLR and tides, and episodic flooding from coastal extremes. The analysis is based on the modular framework LISCOAST (Large-scale Integrated Sea-level and Coastal Assessment Tool). It combines state-of-the-art large-scale modelling tools and datasets to quantify hazard, exposure and vulnerability in coastal areas and compute consequent risks^{37,43}. We considered the five principal SSP scenarios that span a range from ambitious mitigation to no emission policies: SSP1–1.9 that allows achieving the Paris Agreement goal of holding the increase in global temperature to below 1.5 °C compared with pre-industrial levels; low-emissions (SSP1–2.6), reaching net-zero emissions after 2050 and achieving the 2 °C goal; moderate emissions (SSP2–4.5), implying stable emissions until mid-century, when they start to be reduced without reaching net-zero; high emissions (SSP3–7.0), with emissions rising constantly to almost double from current levels by the end of the century; and a high fossil-fuel development world throughout the twenty-first century (SSP5–8.5)⁴⁴. For each of these scenarios, we generated probabilistic projections of mean and extreme sea levels that give rise to permanent inundation or episodic flooding, and combine them with exposure and vulnerability to quantify economic losses. More details on the different steps of the analysis are provided below.

Hazard modelling

Coastal areas in SIDS are exposed to rising mean sea levels (MSL) and episodic high sea levels under extreme atmospheric conditions. ESLs are driven by the combined effect of MSL, tides and water-level fluctuations due to waves and storm surges. We derived the contribution of each of these drivers with state-of-the-art modelling tools and datasets, and combined them to obtain ESLs every 1 km along the coastline.

For the baseline period spanning from 1980 to 2020, we ran a reanalysis of waves and storm surges on the basis of a two-way coupled ocean model using an unstructured grid with a resolution ranging from -50 km offshore to -2 km nearshore. The coupled model system includes the Semi-implicit Cross-scale Hydrosience Integrated System Model (SCHISM)⁴⁵, configured in its 2D barotropic mode and the third-generation spectral wave model (WWM-V)⁴⁶. The model accounts for the combined effects of wind, atmospheric pressure gradients and tides. Bathymetric data are available from the European Marine Observation and Data Network (EMODnet) in angular coordinates at a resolution of 1/8 arc-minute (0.0021° of latitude and longitude; <http://www.emodnet.eu/bathymetry>) and are interpolated onto the computational grid.

We applied the coupled model to produce a reanalysis of waves and storm surges, forced by sea-level pressure and wind speed data from ERA5 (ref. 47). The reanalysis was carried out without tidal forcing to make sure that our hindcast resolves the weather-driven component of ESLs without the stochastic modulation of tidal variations. Further details about the model setup and the validation can be found in ref. 48. Since it is known that nonlinear interactions between tides, waves and storm surges can be important in some areas, we applied a correction for the above effects following an approach similar to that in ref. 49. To this end, we ran a shorter 10-yr reanalysis including tidal forces and from the overlapping time series, we used copulas to produce a correction function for nonlinear tidal effects on water-level anomaly and significant wave height.

To improve the accuracy of the reanalysis data, we implemented some additional steps as detailed below. Using satellite altimetry data, we applied a quantile mapping bias correction on both the water-level anomaly and the significant wave height. This was done after compiling all coinciding model and satellite values along $1^\circ \times 1^\circ$ cells. To further improve the cyclone-related storm surge estimates which have not been sufficiently resolved by our reanalysis, we did additional simulations of tropical cyclone-driven sea-level anomalies using the Delft3D-FM model⁵⁰ forced by the IBTrACS best-track archive⁵¹. The reanalysis values were corrected by considering the tropical cyclone runs values when they are higher than those of our ERA5 runs. More information about the approach and data can be found in ref. 15.

Spectral wave parameters provide one characteristic estimate for wave height, direction and period from the whole spectrum and therefore lack the detail needed to describe wave processes along complex shorelines. To overcome this shortcoming, we used the spectral peaks from the WWM-V model output and propagated each peak along a global transect dataset with 1 km alongshore resolution. The transect dataset includes information on the shoreline position, orientation, submerged and subaerial slope, among others. Details of the data and methods used to generate transects are provided in ref. 52. We benefited from the complete spectral information from the wave model to propagate each peak at each time stamp along its corresponding transect using Snell's law⁵³. We then estimated the wave breaking height combining the peak wave parameters with the submerged profile slope⁵³. Subsequently, we obtained the wave run-up height R_2 on the basis of the Stockdon empirical formula⁵⁴, after combining the breaking wave height and period with the subaerial beach profile slope. The above steps resulted in wave run-up height estimates for each spectral peak and we considered the highest value as the characteristic for the specific time stamp. We then combined the wave run-up with the storm surge to obtain the meteorological tide and applied non-stationary

extreme value analysis⁵⁵ to the time series to obtain estimates for different return periods.

Several of the SIDS coastlines are characterized by the presence of coral reefs and mangroves, which can attenuate nearshore extreme sea levels. Previous studies provide information about the spatial distribution of coral reefs⁵⁶ and mangroves⁵⁷, as well as nearshore extreme sea-level estimates, with and without ecosystem attenuation for different return periods. The latter allowed us to obtain ESL reduction coefficients due to the natural protection from ecosystems, which in turn allowed us to have the final ESLs considering such protection. To assess the importance of natural protection, we carried out a sensitivity analysis applying our framework with and without ecosystem effects for the 50 yr return period event and the baseline, as well as the year 2050 under SSP5-8.5.

Present-day ESLs were produced by combining the final meteorological tide time series with tidal elevations obtained from the FES2014 model⁵⁸. Following the approach in ref. 15, the high-tide water level was considered, taking into account the range due to the spring-neap tide cycle.

We obtained projections of ESLs up to 2100 for the SSP scenarios as follows. Relative SLR projections were obtained from the latest IPCC AR6 assessment^{1,59} and incorporated the effects of the various components of future SLR, as simulated by climate models from the Coupled Model Intercomparison Project phase 6 (CMIP6), including steric SLR, dynamic sea-level change, contributions from glaciers and ice caps, land-water storage and glacial isostatic adjustment, among others. Delft3D-FM⁵⁰ was used to assess changes in global tidal elevations due to changing sea levels¹⁵. Future sea water-level fluctuations due to climate extremes, that is, water levels driven by waves and storm surges, have been shown to be highly uncertain along coastlines worldwide and that they are much smaller than the effects of SLR for moderate and high greenhouse gas emissions trajectories¹⁵. In view of this uncertainty and similar to other global impact studies, projected regional relative SLR was combined with the present meteorological tide estimates to obtain ESLs for future time periods.

All ESL components (RSLR, tide, surges and R_2) were expressed as probability density functions (PDFs) that account for the different sources of uncertainty, and they were combined through Monte Carlo simulations to generate probabilistic estimates of ESLs in each coastal segment (1 km alongshore resolution). Non-stationary extreme value analysis⁵⁵ was then applied to obtain, for a range of return periods (that is, 1, 2, 5, 10, 20, 50, 100, 200, 500, 1,000 and 5,000 yr), PDFs of the corresponding return values of ESL throughout this century.

Previous global or SIDS studies produced inundation maps using static approaches, which are known to overestimate coastal flooding, especially for flat terrains⁶⁰. A substantial improvement of this study is that hydraulic 2D simulations were used along the entire coastline of SIDS to estimate inundation extent and depth. We followed the approach presented in ref. 60 and ran the Lisflood-ACC model⁶¹ at 30 m spatial resolution, using the estimated ESLs as forcing and considering hydraulic roughness derived from land-use maps⁶². Up to high-tide water levels (that is, combination of mean sea level and high tide), we applied the bathtub approach, and land below this sea water level and the corresponding assets were considered permanently inundated due to the effects of sea-level rise. For episodic flooding, Lisflood-ACC was applied for each coastal segment, with the model domain extending up to 200 km landwards to ensure the inclusion of all potentially hydrologically connected areas that may lie inland and away from the coast.

Another improvement compared to previous studies relates to the Digital Elevation Model (DEM) used here, as the accuracy of the DEM used in flood modelling has been identified as one of the major sources of uncertainty in flood inundation modelling^{63,64}. Here we used the recently published GLO-30 DEM⁶⁵ that is based on synthetic aperture radar measurements and is known to reduce the vertical bias of SRTM-based products. In addition, we applied post-processing using

global LIDAR observations to further remove vertical bias, correcting for buildings and vegetation. The description of the development of the new DEM is beyond the scope of the present study but is detailed in ref. 66 and the dataset is publicly available.

Another known limitation of flood risk analyses, especially at regional scale and beyond, is the absence of information on coastal flood protection. As a result, previous studies did not consider protection standards⁶⁷, or used proxy variables such as per capita wealth⁶⁸ or population density and expert judgement⁶⁹. Here we extended the set of criteria and combined a range of indicators as a proxy to define present levels of flood protection at coastal segment resolution. These are: wealth expressed by GDP per capita⁷⁰ considering the World Bank classification (<https://blogs.worldbank.org/opendata/new-world-bank-country-classifications-income-level-2020-2021>), the presence of critical infrastructure such as ports (https://geonode.wfp.org/layers/esri_gn:geonode:wld_trs_ports_wfp) and airports (<https://www.partow.net/miscellaneous/airportdatabase>), urbanization/artificial surface derived from land use and population density (see the following section for the datasets; <http://www.worldpop.org/>).

For each coastal segment, we identified the presence of people, urbanization, critical infrastructure and economic capacity in the present 1-in-500 yr flood area and assumed a positive relation between coastal protection and the number of people, assets and economic activity present in this area⁶⁸. We imposed the following rules to define coastal protection, where the GDP_{capita} refers to the average gridded GDP_{capita} in the coastal segment and not the country GDP_{capita} . The minimum protection level considered was against a 1-in-1 yr sea level. When more than one of the conditions below were satisfied, the higher protection level was chosen. If the 1-in-500 yr flood area of the segment was covered by at least 10% of artificial surface or has a population density >500 people per km^2 , it was assumed that low ($GDP_{capita} < US\$1,036$), lower-middle ($US\$1,036 < GDP_{capita} < US\$4,045$), upper-middle ($US\$4,045 < GDP_{capita} < US\$12,535$) and high-income coastal communities ($GDP_{capita} > US\$12,535$) would be protected against the 1-in-1, 1-in-2, 1-in-5 and 1-in-30 yr ESL, respectively. If there is a large port present, in high-income communities the segment was assumed to be protected up to the 1-in-50 yr event, whereas for the other income societies, protection was up to the 1-in-10 yr event. For small ports, protection was assumed to be either up to a 1-in-2 yr (low, lower-middle income) or a 1-in-10 yr (upper-middle, high income) event. If there is an airport, it was assumed that low, lower-middle, upper-middle and high-income communities would at least be protected for the 1-in-2, 1-in-5, 1-in-10 and 1-in-30 yr ESLs, respectively. Thus, obtained protection levels were implemented in the flood inundation modelling by assuming that flooding occurs only when coastal water level exceeds the existing protection levels. In areas where we obtained unrealistic results, despite the above improvements, we followed the procedure in ref. 43 by applying a reverse calibration of the coastal protection standards using information from the PCRAFI dataset⁷¹, local studies^{12,13,63} and expert judgement.

Exposure and vulnerability

The resulting flood inundation maps were combined with exposure and vulnerability information to estimate population exposure and direct flood damages^{43,72}. For today's population exposure, we overlaid the present inundation maps with the WorldPop 2020 population dataset (www.worldpop.org), which is an open and high-resolution geospatial dataset of population and demographic dynamics, with a focus on low- and middle-income countries. The vulnerability to flooding was expressed through depth-damage functions (DDFs)⁴³, which define the relation between direct damage and flood inundation depth for different land-use classes. Asset values were further scaled according to the GDP per capita available at 5 arc-min resolution⁷⁰ to account for differences in the spatial distribution of wealth within countries.

Baseline global land cover is available from the European Space Agency (<https://worldcover2020.esa.int/>; reference year 2020) at 10 m resolution. Given that more than 95% of the damages relate to built-up areas, land use was corrected to take into account 30-m-resolution gridded information on global human built-up and settlement extent⁷³ (reference year 2010).

Future population exposure for the SSP scenarios was obtained from global projections of population density and urban population gridded at 1 km resolution (<https://sedac.ciesin.columbia.edu/data/set/popdynamics-1-km-downscaled-pop-base-year-projection-ssp-2000-2100-rev01>). Given that urban land-use classes drive most of the estimated coastal flood damages, and in the absence of high-resolution gridded land-use projections, changes in urbanization were used to estimate changes in damages due to land-use change. The projections of urban population were considered as a proxy for the degree of urbanization. Country-level GDP projections for the SSPs were taken from IIASA and OECD⁷⁴. The projected changes in country GDP were spatially disaggregated on the basis of the population projections and were used to adjust future asset values.

Some SIDS were not included in the SSP projections and the missing data were compensated for by values from the most similar countries. To this end, we applied a *k*-means clustering algorithm for all countries using the following variables: the mean latitude and longitude of the country border polygon, GDP, GDP per capita, population, country area and population. The algorithm grouped all countries into 20 clusters on the basis of similarities in their location and socioeconomic characteristics. For each SIDS not included in the SSP projections, we considered the average relative change of all countries belonging to the same cluster.

Risk assessment

For each coastal segment, the area flooded, number of people affected and direct flood losses were calculated at ~100 m resolution by combining flood inundation estimates with population and land-use maps, and the vulnerability functions. For areas that are inundated on a regular basis (which could happen in the future with SLR), defined as lying below the present high-tide water level, assets were considered as fully damaged and the maximum loss according to the DDFs was applied. For areas inundated only during extreme events, the damage was estimated by applying the DDFs combined with the simulated inundation depth and land-use information.

MSLs and ESLs, and the corresponding flood depths, are available as PDFs for different return periods (1, 2, 5, 10, 20, 50, 100, 200, 500, 1,000 and 5,000 yr). Consequently, for each coastal segment, we obtained probabilistic estimates of flooded area (FA), population exposed (PE) and impact (D) from 1981 up to 2100. Integrating FA, PE and D over the return periods allowed obtaining the EAFA, EAPE and EAD. We present and discuss our results on risk at global, regional, as well as country level, and we focus on the median, 5th and 95th percentiles (very likely range).

Adaptation

Even though assessing adaptation options lies beyond the scope of the present study, we produced preliminary results about the additional protection height needed to keep the 2100 EAD at present-day levels. To this end, we estimated the 2100 EAD by incrementally increasing the protection standard and producing curves of EAD as a function of the coastal protection standard. These curves were then interpolated to estimate the protection needed to achieve the desired EAD, which is expressed in return periods, additional elevation, as well as cost per km of coastline, with unit costs available from previous studies³⁷.

Limitations

The present study expresses the current state of the art in large-scale coastal impact assessments, but the spatial and temporal scales

considered impose some inevitable epistemic and data limitations. We focused on direct damages from flooding and excluded indirect damages. The latter can be substantial but require a different modelling framework⁷⁵ and are beyond the scope of our study.

ESLs are the combined result of rising sea levels, tides, waves and storm surge which are known to interact with each other⁴⁹. With the two-way coupled model used here, we resolved the sensitivity of wave processes to ocean circulation and storm surge⁷⁶, as well as the Doppler and other effects of tidal and wind-driven currents to waves⁷⁷. On the other hand, we omitted nonlinear interactions between SLR and the other ESL components²⁷. This is an inherent limitation of present state-of-the-art large-scale assessments, as discussed in detail in ref. 15 and other studies^{78,79}.

Our work advances in the estimation of wave run-up to express wave contributions to ESLs, compared with the generic approximation of wave set-up previously applied^{43,60,79}. This was feasible due to recently published datasets of submerged and subaerial beach profile slopes. On the other hand, we omitted other wave-related processes such as overtopping⁸⁰ and coastal protection failure⁸¹. This would require very detailed simulations that are presently not feasible at this scale.

Nearshore hydrodynamic processes are modulated by the constantly changing nearshore topography and bathymetry⁸², and events of similar intensity occurring a few days apart can have distinctly different impacts on the coast due to changing wave attenuation patterns⁸³. Such complexity can be even more enhanced in coral atolls^{11,21,23} and other environments where geological controls can affect nearshore hydrodynamics and sediment transport^{84,85}. Simulating the above interactions requires high-resolution process-based models and data^{21–23}. Performing such detailed analysis in a common framework for all SIDS is currently infeasible due to a lack of detailed data for all SIDS and computational restrictions. Even if these limitations were somehow overcome, issues arising from the uncertainty in future geomorphological conditions still remain. Climate change and rising seas, long-term weather variability and human interventions will affect nearshore morphology in a way that is difficult to predict⁸⁶. As coastal morphology evolves, especially under rising seas⁸⁷, the range of possible future topo-bathymetric conditions that could govern nearshore extreme sea levels²⁷ becomes very broad and prohibits the application of expensive modelling frameworks at large scales.

Despite continued efforts to improve coastal protection characterization, we recognize that the scientific community is still a long way away from having accurate information regarding protection standards along the global coastlines, including those of SIDS⁶⁴. We used wealth as a proxy for vulnerability in line with empirical evidence that shows a strong relation between wealth and socioeconomic impact³⁰. Even though our estimates are based on gridded data, hence trying to capture local differences between and within countries, existing wealth inequalities can result in artefacts when considering the GDP per capita as a proxy for the interplay between risk perception and coastal protection. For transparency, the protection standards applied in this research are made available together with the public dataset to facilitate similar assessments and possible improvements whenever new information becomes available. An additional known important factor of uncertainty is the digital elevation model, which albeit improved compared to previous efforts, still introduce epistemic uncertainty in our framework.

Reporting summary

Further information on research design is available in the Nature Portfolio Reporting Summary linked to this article.

Data availability

The models and datasets presented are part of the integrated risk assessment tool LISCoAsT (Large-scale Integrated Sea-level and Coastal Assessment Tool) developed by the Joint Research Centre of

the European Commission. The flood risk assessment data are provided in the supplementary information. Source data are provided with this paper.

Code availability

Most of the code that supported the findings of this study is already open access, with references provided in the manuscript; specific tools that are not available in public repositories will be available on reasonable request from the corresponding authors.

References

- Garner, G. G. et al. *IPCC AR6 Sea-Level Rise Projections, Version 20210809* (DAAC, CA, USA, 2021).
- Morim, J., Hemer, M., Cartwright, N., Strauss, D. & Andutta, F. On the concordance of 21st century wind-wave climate projections. *Glob. Planet. Change* **167**, 160–171 (2018).
- Hinkel, J. et al. Coastal flood damage and adaptation costs under 21st century sea-level rise. *Proc. Natl Acad. Sci. USA* **111**, 3292–3297 (2014).
- IPCC. *Climate Change: The IPCC Scientific Assessment* (Cambridge Univ. Press, 1990).
- Oppenheimer, M. et al. in *IPCC Special Report on the Ocean and Cryosphere in a Changing Climate* (eds Pörtner, H.-O. et al.) 321–445 (Cambridge Univ. Press, 2019).
- Mycioo, M. A. Beyond 1.5°C: vulnerabilities and adaptation strategies for Caribbean Small Island Developing States. *Reg. Environ. Change* **18**, 2341–2353 (2018).
- Leal Filho, W. et al. Climate change adaptation on small island states: an assessment of limits and constraints. *J. Mar. Sci. Eng.* **9**, 602 (2021).
- Mycioo, M. et al. in *Climate Change 2022: Impacts, Adaptation and Vulnerability* (eds Pörtner, H.-O. et al.) 2043–2121 (Cambridge Univ. Press, 2022).
- Deopersad, C. et al. *Assessment of the Effects and Impacts of Hurricane Dorian in the Bahamas* (Inter-American Developmental Bank, 2020).
- Post-disaster Needs Assessment Hurricane Maria September 18, 2017* (Government of Dominica, 2017).
- Albert, S. et al. Interactions between sea-level rise and wave exposure on reef island dynamics in the Solomon Islands. *Environ. Res. Lett.* **11**, 054011 (2016).
- Giardino, A., Nederhoff, K. & Vousdoukas, M. Coastal hazard risk assessment for small islands: assessing the impact of climate change and disaster reduction measures on Ebeye (Marshall Islands). *Reg. Environ. Change* **18**, 2237–2248 (2018).
- Monioudi, I. N. et al. Climate change impacts on critical international transportation assets of Caribbean Small Island Developing States (SIDS): the case of Jamaica and Saint Lucia. *Reg. Environ. Change* **18**, 2211–2225 (2018).
- Reyer, C. P. O. et al. Climate change impacts in Latin America and the Caribbean and their implications for development. *Reg. Environ. Change* **17**, 1601–1621 (2017).
- Vousdoukas, M. I. et al. Global probabilistic projections of extreme sea levels show intensification of coastal flood hazard. *Nat. Commun.* **9**, 2360 (2018).
- Magnan, A. K. et al. Sea level rise risks and societal adaptation benefits in low-lying coastal areas. *Sci. Rep.* **12**, 10677 (2022).
- Tiggeloven, T. et al. Global-scale benefit–cost analysis of coastal flood adaptation to different flood risk drivers using structural measures. *Nat. Hazards Earth Syst. Sci.* **20**, 1025–1044 (2020).
- Powell, E. J., Tyrrell, M. C., Milliken, A., Tirpak, J. M. & Staudinger, M. D. A review of coastal management approaches to support the integration of ecological and human community planning for climate change. *J. Coast. Conserv.* **23**, 1–18 (2019).

19. Dellink, R., Chateau, J., Lanzi, E. & Magné, B. Long-term economic growth projections in the Shared Socioeconomic Pathways. *Glob. Environ. Change* **42**, 200–214 (2017).
20. Robinson, S.-A. Climate change adaptation in SIDS: a systematic review of the literature pre and post the IPCC Fifth Assessment Report. *WIREs Clim. Change* **11**, e653 (2020).
21. Storlazzi, C. D. et al. Most atolls will be uninhabitable by the mid-21st century because of sea-level rise exacerbating wave-driven flooding. *Sci. Adv.* **4**, eaap9741 (2018).
22. Amores, A., Marcos, M., Le Cozannet, G. & Hinkel, J. Coastal flooding and mean sea-level rise allowances in atoll island. *Sci. Rep.* **12**, 1281 (2022).
23. Beetham, E. & Kench, P. S. Predicting wave overtopping thresholds on coral reef-island shorelines with future sea-level rise. *Nat. Commun.* **9**, 3997 (2018).
24. Carlot, J. et al. Coral reef structural complexity loss exposes coastlines to waves. *Sci. Rep.* **13**, 1683 (2023).
25. Mentaschi, L., Vousdoukas, M. I., Pekel, J.-F., Voukouvalas, E. & Feyen, L. Global long-term observations of coastal erosion and accretion. *Sci. Rep.* **8**, 12876 (2018).
26. Ranasinghe, R. On the need for a new generation of coastal change models for the 21st century. *Sci. Rep.* **10**, 2010 (2020).
27. Du, J. et al. Tidal response to sea-level rise in different types of estuaries: the importance of length, bathymetry, and geometry. *Geophys. Res. Lett.* **45**, 227–235 (2018).
28. Bisaro, A., de Bel, M., Hinkel, J., Kok, S. & Bouwer, L. M. Leveraging public adaptation finance through urban land reclamation: cases from Germany, the Netherlands and the Maldives. *Clim. Change* **160**, 671–689 (2020).
29. Bouwer, L. M. & Jonkman, S. N. Global mortality from storm surges is decreasing. *Environ. Res. Lett.* **13**, 014008 (2018).
30. Formetta, G. & Feyen, L. Empirical evidence of declining global vulnerability to climate-related hazards. *Glob. Environ. Change* **57**, 101920 (2019).
31. Aerts, J. C. J. H. et al. Integrating human behaviour dynamics into flood disaster risk assessment. *Nat. Clim. Change* **8**, 193–199 (2018).
32. Hughes, T. P. et al. Coral reefs in the Anthropocene. *Nature* **546**, 82–90 (2017).
33. Saintilan, N. et al. Widespread retreat of coastal habitat is likely at warming levels above 1.5°C. *Nature* **621**, 112–119 (2023).
34. Stovall, A. E. et al. *Coral Reef Restoration for Risk Reduction (CR4): A Guide to Project Design and Proposal Development* (US Coral Reef Task Force, 2022); https://www.coralreef.gov/assets/about/cr4_guide_nov2022_508.pdf
35. Thomas, A., Serdeczny, O. & Pringle, P. Loss and damage research for the global stocktake. *Nat. Clim. Change* **10**, 700 (2020).
36. Ourbak, T. & Magnan, A. K. The Paris Agreement and climate change negotiations: small islands, big players. *Reg. Environ. Change* **18**, 2201–2207 (2018).
37. Vousdoukas, M. I. et al. Economic motivation for raising coastal flood defenses in Europe. *Nat. Commun.* **11**, 2119 (2020).
38. Temmerman, S. et al. Ecosystem-based coastal defence in the face of global change. *Nature* **504**, 79–83 (2013).
39. Beck, M. W. et al. Return on investment for mangrove and reef flood protection. *Ecosyst. Serv.* **56**, 101440 (2022).
40. Seddon, N. et al. Global recognition of the importance of nature-based solutions to the impacts of climate change. *Glob. Sustain.* **3**, e15 (2020).
41. Sasmito, S. D., Murdiyarso, D., Friess, D. A. & Kurnianto, S. Can mangroves keep pace with contemporary sea level rise? A global data review. *Wetl. Ecol. Manage.* **24**, 263–278 (2016).
42. Gussmann, G. & Hinkel, J. What drives relocation policies in the Maldives? *Clim. Change* **163**, 931–951 (2020).
43. Vousdoukas, M. I. et al. Climatic and socioeconomic controls of future coastal flood risk in Europe. *Nat. Clim. Change* **8**, 776–780 (2018).
44. Meinshausen, M. et al. The shared socio-economic pathway (SSP) greenhouse gas concentrations and their extensions to 2500. *Geosci. Model Dev.* **13**, 3571–3605 (2020).
45. Zhang, Y. J., Ye, F., Stanev, E. V. & Grashorn, S. Seamless cross-scale modeling with SCHISM. *Ocean Modell.* **102**, 64–81 (2016).
46. Roland, A. et al. A fully coupled 3D wave-current interaction model on unstructured grids. *J. Geophys. Res. Oceans* **117**, 2156–2202 (2012).
47. Hersbach, H. et al. The ERA5 global reanalysis. *Q. J. R. Meteorol. Soc.* **146**, 1999–2049 (2020).
48. Mentaschi, L. et al. A global unstructured, coupled, high-resolution hindcast of waves and storm surge. *Front. Mar. Sci.* <https://doi.org/10.3389/fmars.2023.1233679> (2023)
49. Arns, A. et al. Non-linear interaction modulates global extreme sea levels, coastal flood exposure, and impacts. *Nat. Commun.* **11**, 1918 (2020).
50. Muis, S., Verlaan, M., Winsemius, H. C., Aerts, J. C. J. H. & Ward, P. J. A global reanalysis of storm surges and extreme sea levels. *Nat. Commun.* **7**, 11969 (2016).
51. Knapp, K. R., Kruk, M. C., Levinson, D. H., Diamond, H. J. & Neumann, C. J. The International Best Track Archive for Climate Stewardship (IBTrACS). *Bull. Am. Meteorol. Soc.* **91**, 363–376 (2010).
52. Athanasiou, P. et al. Global database of Coastal Characteristics (GCC) (1.0). Zenodo <https://doi.org/10.5281/zenodo.8200200> (2023).
53. *Coastal Engineering Manual* (US Army Corps of Engineers, 2002).
54. Stockdon, H. F., Holman, R. A., Howd, P. A. & Sallenger, J. A. H. Empirical parameterization of setup, swash, and runup. *Coast. Eng.* **53**, 573–588 (2006).
55. Mentaschi, L. et al. Non-stationary Extreme Value Analysis: a simplified approach for Earth science applications. *Hydrol. Earth Syst. Sci. Discuss.* <https://doi.org/10.5194/hess-2016-65> (2016).
56. Beck, M. W. et al. The global flood protection savings provided by coral reefs. *Nat. Commun.* **9**, 2186 (2018).
57. Menéndez, P., Losada, I. J., Torres-Ortega, S., Narayan, S. & Beck, M. W. The global flood protection benefits of mangroves. *Sci. Rep.* **10**, 4404 (2020).
58. Carrere, L., Lyard, F., Cancet, M., Guillot, A., Picot, N. FES 2014, a new tidal model: validation results and perspectives for improvements. In *ESA Living Planet Conference* (Prague, 2016).
59. Fox-Kemper, B. et al. in *Climate Change 2021: The Physical Science Basis* (eds Masson-Delmotte, V. et al.) 1211–1362 (Cambridge Univ. Press, 2021).
60. Vousdoukas, M. I. et al. Developments in large-scale coastal flood hazard mapping. *Nat. Hazards Earth Syst. Sci.* **16**, 1841–1853 (2016).
61. Bates, P. D., Horritt, M. S. & Fewtrell, T. J. A simple inertial formulation of the shallow water equations for efficient two-dimensional flood inundation modelling. *J. Hydrol.* **387**, 33–45 (2010).
62. *CCI Land Cover Time-Series v2.0.7 (1992–2015)* (European Space Agency, 2010); <https://www.esa-landcover-cci.org/>
63. Bove, G., Becker, A., Sweeney, B., Vousdoukas, M. & Kulp, S. A method for regional estimation of climate change exposure of coastal infrastructure: case of USVI and the influence of digital elevation models on assessments. *Sci. Tot. Environ.* **710**, 136162 (2020).
64. Vousdoukas, M. I. et al. Understanding epistemic uncertainty in large-scale coastal flood risk assessment for present and future climates. *Nat. Hazards Earth Syst. Sci.* **18**, 2127–2142 (2018).
65. *Copernicus Digital Elevation Model. Product Handbook* (Airbus, 2020).
66. Pronk, M. et al. DeltaDEM: a global coastal digital terrain model. Public dataset <https://doi.org/10.4121/21997565> (2023).

67. Kirezci, E. et al. Projections of global-scale extreme sea levels and resulting episodic coastal flooding over the 21st Century. *Sci. Rep.* **10**, 11629 (2020).
68. Scussolini, P. et al. FLOPROS: an evolving global database of flood protection standards. *Nat. Hazards Earth Syst. Sci.* **16**, 1049–1061 (2016).
69. Lincke, D. & Hinkel, J. Economically robust protection against 21st century sea-level rise. *Glob. Environ. Change* **51**, 67–73 (2018).
70. Kummu, M., Taka, M. & Guillaume, J. H. A. Gridded global datasets for Gross Domestic Product and Human Development Index over 1990–2015. *Sci. Data* **5**, 180004 (2018).
71. PCRAFI. Pacific Catastrophe Risk Assessment and Financing Initiative. in: *Programme* (ed. SotPRE) (2022).
72. Boettle, M., Rybski, D. & Kropp, J. P. Quantifying the effect of sea level rise and flood defence – a point process perspective on coastal flood damage. *Nat. Hazards Earth Syst. Sci.* **16**, 559–576 (2016).
73. Wang, P., Huang, C., Brown de Colstoun, E. C., Tilton, J. C., Tan, B. Global Human Built-up and Settlement Extent (HBASE) dataset from Landsat (ed. NSDaAC). (SEDAC, Palisades, NY, 2017).
74. O’Neill, B. C. et al. A new scenario framework for climate change research: the concept of shared socioeconomic pathways. *Clim. Change* **122**, 387–400 (2014).
75. Schinko, T. et al. Economy-wide effects of coastal flooding due to sea level rise: a multi-model simultaneous treatment of mitigation, adaptation, and residual impacts. *Environ. Res. Commun.* **2**, 015002 (2020).
76. Bertin, X., Li, K., Roland, A. & Bidlot, J.-R. The contribution of short-waves in storm surges: two case studies in the Bay of Biscay. *Cont. Shelf Res.* **96**, 1–15 (2015).
77. Dodet, G. et al. Wave-current interactions in a wave-dominated tidal inlet. *J. Geophys. Res. Oceans* **118**, 1587–1605 (2013).
78. Vousdoukas, M. I., Voukouvalas, E., Annunziato, A., Giardino, A. & Feyen, L. Projections of extreme storm surge levels along Europe. *Clim. Dyn.* **47**, 3171–3190 (2016).
79. Vousdoukas, M. I., Mentaschi, L., Voukouvalas, E., Verlaan, M. & Feyen, L. Extreme sea levels on the rise along Europe’s coasts. *Earths Future* <https://doi.org/10.1002/2016EF000505> (2017).
80. Matias, A., Ferreira, Ó., Vila-Concejo, A., Garcia, T. & Dias, J. A. Classification of washover dynamics in barrier islands. *Geomorphology* **97**, 655–674 (2008).
81. Oumeraci, H. Review and analysis of vertical breakwater failures—lessons learned. *Coast. Eng.* **22**, 3–29 (1994).
82. Qi, H., Cai, F., Lei, G., Cao, H. & Shi, F. The response of three main beach types to tropical storms in South China. *Mar. Geol.* **275**, 244–254 (2010).
83. Vousdoukas, M. I., Almeida, L. P. & Ferreira, Ó. Beach erosion and recovery during consecutive storms at a steep-sloping, meso-tidal beach. *Earth Surf. Process. Landf.* **37**, 583–691 (2012).
84. Gallop, S. L., Bosserelle, C., Pattiaratchi, C. & Eliot, I. Rock topography causes spatial variation in the wave, current and beach response to sea breeze activity. *Mar. Geol.* **290**, 29–40 (2011).
85. Vousdoukas, M. I. et al. Field observations and modeling of wave attenuation over colonized beachrocks. *Cont. Shelf Res.* **48**, 100–109 (2012).
86. Athanasiou, P. et al. Uncertainties in projections of sandy beach erosion due to sea level rise: an analysis at the European scale. *Sci. Rep.* **10**, 11895 (2020).
87. Schuerch, M. et al. Future response of global coastal wetlands to sea-level rise. *Nature* **561**, 231–234 (2018).

Acknowledgements

R.E.K. was supported by US National Science Foundation award ICER-2103754 as part of the Megalopolitan Coastal Transformation Hub and by the US National Aeronautics and Space Administration (award 80NSSC20K1724 and JPL task 105393.509496.02.08.13.31). M.W.B. received support from NSF 2209284-Strong Coasts, AXA Research Fund and the Center for Coastal Climate Resilience (M.W.B., P.M.). R.R. was partly supported by the AXA Research Fund. We thank the sea-level projection authors for developing and making the sea-level rise projections available, multiple funding agencies for supporting the development of the projections, and the NASA Sea-Level Change Team for developing and hosting the IPCC AR6 Sea-Level Projection Tool. The views expressed in the article do not reflect the views of ADB.

Author contributions

M.I.V., A.G., L.M., R.R. and L.F. conceptualized the project. M.I.V., P.A., A.G., L.M., R.E.K., P.M. and M.W.B. performed preliminary and exploratory analysis. M.I.V., R.R. and L.F. developed the methodology. M.I.V., P.A., A.G., L.M., A.S., R.E.K., P.M., R.R. and M.W.B. conducted validation. M.I.V. performed formal analysis, investigation and visualization. M.I.V. and L.F. acquired resources. M.I.V., L.M. and P.M. performed data integration. M.I.V. and L.F. wrote the original draft, which all authors reviewed and edited.

Competing interests

The authors declare no competing interests.

Additional information

Supplementary information The online version contains supplementary material available at <https://doi.org/10.1038/s41893-023-01230-5>.

Correspondence and requests for materials should be addressed to Michalis I. Vousdoukas or Luc Feyen.

Peer review information *Nature Sustainability* thanks Bruce Glavovic, Carl-Friedrich Schleussner and the other, anonymous, reviewer(s) for their contribution to the peer review of this work.

Reprints and permissions information is available at www.nature.com/reprints.

Publisher’s note Springer Nature remains neutral with regard to jurisdictional claims in published maps and institutional affiliations.

Open Access This article is licensed under a Creative Commons Attribution 4.0 International License, which permits use, sharing, adaptation, distribution and reproduction in any medium or format, as long as you give appropriate credit to the original author(s) and the source, provide a link to the Creative Commons license, and indicate if changes were made. The images or other third party material in this article are included in the article’s Creative Commons license, unless indicated otherwise in a credit line to the material. If material is not included in the article’s Creative Commons license and your intended use is not permitted by statutory regulation or exceeds the permitted use, you will need to obtain permission directly from the copyright holder. To view a copy of this license, visit <http://creativecommons.org/licenses/by/4.0/>.

© The Author(s) 2023

Reporting Summary

Nature Portfolio wishes to improve the reproducibility of the work that we publish. This form provides structure for consistency and transparency in reporting. For further information on Nature Portfolio policies, see our [Editorial Policies](#) and the [Editorial Policy Checklist](#).

Statistics

For all statistical analyses, confirm that the following items are present in the figure legend, table legend, main text, or Methods section.

n/a Confirmed

- The exact sample size (n) for each experimental group/condition, given as a discrete number and unit of measurement
- A statement on whether measurements were taken from distinct samples or whether the same sample was measured repeatedly
- The statistical test(s) used AND whether they are one- or two-sided
Only common tests should be described solely by name; describe more complex techniques in the Methods section.
- A description of all covariates tested
- A description of any assumptions or corrections, such as tests of normality and adjustment for multiple comparisons
- A full description of the statistical parameters including central tendency (e.g. means) or other basic estimates (e.g. regression coefficient) AND variation (e.g. standard deviation) or associated estimates of uncertainty (e.g. confidence intervals)
- For null hypothesis testing, the test statistic (e.g. F , t , r) with confidence intervals, effect sizes, degrees of freedom and P value noted
Give P values as exact values whenever suitable.
- For Bayesian analysis, information on the choice of priors and Markov chain Monte Carlo settings
- For hierarchical and complex designs, identification of the appropriate level for tests and full reporting of outcomes
- Estimates of effect sizes (e.g. Cohen's d , Pearson's r), indicating how they were calculated

Our web collection on [statistics for biologists](#) contains articles on many of the points above.

Software and code

Policy information about [availability of computer code](#)

Data collection

Data analysis

For manuscripts utilizing custom algorithms or software that are central to the research but not yet described in published literature, software must be made available to editors and reviewers. We strongly encourage code deposition in a community repository (e.g. GitHub). See the Nature Portfolio [guidelines for submitting code & software](#) for further information.

Data

Policy information about [availability of data](#)

All manuscripts must include a [data availability statement](#). This statement should provide the following information, where applicable:

- Accession codes, unique identifiers, or web links for publicly available datasets
- A description of any restrictions on data availability
- For clinical datasets or third party data, please ensure that the statement adheres to our [policy](#)

All data used are public and sources are provided in the manuscript. The final dataset produced is available through the LISCoAsT repository of the JRC data collection (<http://data.jrc.ec.europa.eu/collection/LISCOAST>)

Research involving human participants, their data, or biological material

Policy information about studies with [human participants or human data](#). See also policy information about [sex, gender \(identity/presentation\), and sexual orientation](#) and [race, ethnicity and racism](#).

Reporting on sex and gender	Not relevant
Reporting on race, ethnicity, or other socially relevant groupings	Not relevant
Population characteristics	Not relevant
Recruitment	Not relevant
Ethics oversight	Not relevant

Note that full information on the approval of the study protocol must also be provided in the manuscript.

Field-specific reporting

Please select the one below that is the best fit for your research. If you are not sure, read the appropriate sections before making your selection.

Life sciences Behavioural & social sciences Ecological, evolutionary & environmental sciences

For a reference copy of the document with all sections, see [nature.com/documents/nr-reporting-summary-flat.pdf](https://www.nature.com/documents/nr-reporting-summary-flat.pdf)

Ecological, evolutionary & environmental sciences study design

All studies must disclose on these points even when the disclosure is negative.

Study description	An assessment of coastal flood risk for all SIDS in view of climate change scenarios
Research sample	The framework combines datasets about extreme sea levels, topography, land use, population, socioeconomic data to assess how their interplay will affect future coastal flood losses
Sampling strategy	Not relevant
Data collection	No data collection is involved, all data were previously available
Timing and spatial scale	The time frame is from 1980 until 2100 which is enough to express current and future conditions relevant to key climate change policy and research. The temporal resolution is of 6 hours, enough to resolve major storms. The spatial resolution is 30 m, enough to resolve the dynamics of coastal flooding.
Data exclusions	Not available
Reproducibility	All simulations are deterministic so there are no reproducibility issues.
Randomization	Not relevant
Blinding	Not relevant

Did the study involve field work? Yes No

Field work, collection and transport

Field conditions	Not relevant
Location	Not relevant
Access & import/export	Not relevant
Disturbance	Not relevant

Reporting for specific materials, systems and methods

We require information from authors about some types of materials, experimental systems and methods used in many studies. Here, indicate whether each material, system or method listed is relevant to your study. If you are not sure if a list item applies to your research, read the appropriate section before selecting a response.

Materials & experimental systems

- | n/a | Involvement in the study |
|-------------------------------------|--|
| <input checked="" type="checkbox"/> | <input type="checkbox"/> Antibodies |
| <input checked="" type="checkbox"/> | <input type="checkbox"/> Eukaryotic cell lines |
| <input checked="" type="checkbox"/> | <input type="checkbox"/> Palaeontology and archaeology |
| <input checked="" type="checkbox"/> | <input type="checkbox"/> Animals and other organisms |
| <input checked="" type="checkbox"/> | <input type="checkbox"/> Clinical data |
| <input checked="" type="checkbox"/> | <input type="checkbox"/> Dual use research of concern |
| <input checked="" type="checkbox"/> | <input type="checkbox"/> Plants |

Methods

- | n/a | Involvement in the study |
|-------------------------------------|---|
| <input checked="" type="checkbox"/> | <input type="checkbox"/> ChIP-seq |
| <input checked="" type="checkbox"/> | <input type="checkbox"/> Flow cytometry |
| <input checked="" type="checkbox"/> | <input type="checkbox"/> MRI-based neuroimaging |